TOXICOLOGICAL SCIENCES, 164(2), 2018, 477–488

doi: 10.1093/toxsci/kfy101
Advance Access Publication Date: April 23, 2018
Research Article

# Effect of the Catechol-O-Methyltransferase Inhibitors Tolcapone and Entacapone on Fatty Acid Metabolism in HepaRG Cells

David Grünig,[*,†] Andrea Felser,[*,†,1] Urs Duthaler,[*,†,1] Jamal Bouitbir,[*,†,‡] and Stephan Krähenbühl[*,†,‡,2]

[*]Division of Clinical Pharmacology & Toxicology, University Hospital Basel, 4031 Basel, Switzerland; [†]Department of Biomedicine, University of Basel, 4031 Basel, Switzerland; and [‡]Swiss Center for Applied Human Toxicology (SCAHT), 4055 Basel, Switzerland

[1]These authors contributed equally to this study.
[2]To whom correspondence should be addressed. Fax: +41-61-265-4560. E-mail: kraehenbuehl@uhbs.ch.

## ABSTRACT

Tolcapone and entacapone are catechol-O-methyltransferase inhibitors used in patients with Parkinson's disease. For tolcapone, patients with liver failure have been reported with microvesicular steatosis observed in the liver biopsy of 1 patient. We therefore investigated the impact of tolcapone and entacapone on fatty acid metabolism in HepaRG cells exposed for 24 h and on acutely exposed mouse liver mitochondria. In HepaRG cells, tolcapone induced lipid accumulation starting at 100 μM, whereas entacapone was ineffective up to 200 μM. In HepaRG cells, tolcapone-inhibited palmitate metabolism and activation starting at 100 μM, whereas entacapone did not affect palmitate metabolism. In isolated mouse liver mitochondria, tolcapone inhibited palmitate metabolism starting at 5 μM and entacapone at 50 μM. Inhibition of palmitate activation could be confirmed by the acylcarnitine pattern in the supernatant of HepaRG cell cultures. Tolcapone-reduced mRNA and protein expression of long-chain acyl-CoA synthetase 1 (ACSL1) and protein expression of ACSL5, whereas entacapone did not affect ACSL expression. Tolcapone increased mRNA expression of the fatty acid transporter CD36/FAT, impaired the secretion of ApoB100 by HepaRG cells and reduced the mRNA expression of ApoB100, but did not relevantly affect markers of fatty acid binding, lipid droplet formation and microsomal lipid transfer. In conclusion, tolcapone impaired hepatocellular fatty acid metabolism at lower concentrations than entacapone. Tolcapone increased mRNA expression of fatty acid transporters, inhibited activation of long-chain fatty acids and impaired very low-density lipoprotein secretion, causing hepatocellular triglyceride accumulation. The findings may be relevant in patients with a high tolcapone exposure and preexisting mitochondrial dysfunction.

**Key words:** COMT inhibitors; HepaRG cells; fatty acid metabolism; long-chain acyl-CoA synthetase; VLDL secretion.

Tolcapone and entacapone are catechol-O-methyltransferase (COMT) inhibitors used for the treatment of patients with Parkinson's disease. COMT inhibitors act mainly in the periphery and block O-methylation of DOPA, thereby increasing the availability of DOPA for transport into the brain and decreasing the formation 3-O-methyl-DOPA, which may impair DOPA transport into the brain (Kaakkola, 2000). Treatment with COMT inhibitors usually allows a reduction of the DOPA dose and leads to an increase in the on-time as well as to a decrease in DOPA-associated dyskinesias (Kaakkola, 2000).

In humans, both compounds are almost completely absorbed and have bioavailabilities in the range of 60% (tolcapone) and 35% (entacapone), indicating a significant first liver-pass effect. They are rapidly eliminated with half-lives of 2–3 h. Entacapone is mainly glucuronidated and eliminated almost completely over the bile/feces as the glucuronide or the parent

compound. In comparison, only approximately 30% of tolcapone is glucuronidated and 40% eliminated by the bile/feces (Jorga *et al.*, 2001). In contrast to entacapone, tolcapone can also be O-methylated and undergo oxidative metabolism by cytochrome P450 (CYP) 3A4 and other CYPs. Entacapone is approximately 98% bound to serum proteins and tolcapone >99%. The dosage of entacapone is usually 200 mg together with every dose of L-DOPA (mostly 3 times a day) and of tolcapone 100–200 mg 3 times daily. Maximal plasma concentrations were approximately 6 μM after a single dose of 200 mg entacapone and 17 μM after a single dose of 100 mg tolcapone (Kaakkola, 2000). The liver concentration is not known, but may be higher than in plasma after oral ingestion taking into account the first liver-pass effect.

The most prevalent adverse reactions of the COMT inhibitors mainly reflect dopamine toxicity such as hypotension, nausea, hallucinations and dyskinesias (Haasio, 2010; Kaakkola, 2000). Nondopaminergic adverse reactions mainly include diarrhea and abdominal pain. Hepatocellular liver injury (increased transaminases) has been observed in clinical studies in approximately 3% and 0.2% of patients treated with tolcapone and entacapone, respectively (Haasio, 2010; Kaakkola, 2000; Lew and Kricorian, 2007). Regarding tolcapone, hepatocellular injury is dose-dependent and usually occurs during the first 6 months of treatment (Olanow, 2000). Increased transaminases typically return rapidly to normal after stopping tolcapone, but can also normalize over time in patients with continuous treatment. Four patients with liver failure associated with tolcapone have been described, and 3 of these patients died (Olanow, 2000). In 2 of these patients, a liver biopsy was performed. One of these biopsies revealed centroacinar necrosis with an inflammatory infiltrate in the portal tracts and microvesicular steatosis in adjacent hepatocytes (Assal *et al.*, 1998; Spahr *et al.*, 2000). Electron microscopy of hepatocytes showed proliferation of swollen mitochondria, reduction in matrix density and loss of cristae (Borges, 2003; Spahr *et al.*, 2000), suggesting that tolcapone is a mitochondrial toxicant.

We recently described the toxicity of tolcapone and entacapone on the respiratory chain of mitochondria in HepaRG cells exposed for 24 h and acutely exposed mouse liver mitochondria in detail (Grunig *et al.*, 2017). In that study, tolcapone inhibited the function of enzyme complexes of the electron transport chain and uncoupled oxidative phosphorylation in a concentration-dependent manner. Entacapone showed similar toxic effects, but at clearly higher concentrations. These findings were in agreement with previous studies showing that tolcapone uncouples oxidative phosphorylation of liver mitochondria, leading to a drop in the membrane potential of isolated rat liver mitochondria (Haasio, 2010), and to increased body temperature, weight loss, and hepatotoxicity in rats (Haasio *et al.*, 2001, 2002b). Mitochondrial toxicity of tolcapone was also suggested in a capture compound mass spectrometry study, in which tolcapone interacted preferentially with proteins of the mitochondrial respiratory chain and of fatty acid metabolism (Fischer *et al.*, 2010).

During our recent investigations of mitochondrial function in HepaRG cells (Grunig *et al.*, 2017), we also observed that tolcapone and entacapone inhibited the metabolism of palmitate, suggesting impairment of hepatic fatty acid metabolism. This finding was in agreement with microvesicular steatosis described in the liver biopsy of a patient with tolcapone-associated liver injury (Spahr *et al.*, 2000) and with the interaction of tolcapone and/or tolcapone metabolites with enzymes involved in fatty acid metabolism (Fischer, *et al.*, 2010). We therefore decided to study the effect of the COMT inhibitors tolcapone and entacapone on fatty acid metabolism using HepaRG cells and isolated mouse liver mitochondria in more detail. The studies showed that tolcapone mainly inhibited activation of fatty acids and excretion of very low-density lipoprotein (VLDL), causing hepatocellular lipid accumulation.

## MATERIALS AND METHODS

*Chemicals*. Triacsin C (TC), entacapone (Enta), 4-bromocrotonic acid (4bc) were acquired from Santa Cruz Biotechnology (Dallas, Texas), Toronto Research Chemicals (Toronto, CAN) and TCI Chemicals (Eschborn, Germany), respectively. Tolcapone (Tol), etomoxir (Et), and methylenecyclopropylacetic acid (MCPA) were obtained from Sigma-Aldrich (Buchs, Switzerland). If not stated otherwise, all other chemicals were also purchased from Sigma-Aldrich. Drug or toxicant stock solutions were dissolved in DMSO and kept at −20° C for cell treatment (in general at 1:1000 dilution).

*Cell cultures*. All cells were kept at 37°C in a humidified 5% $CO_2$ cell culture incubator and were passaged using trypsin. Cell culture supplements were all purchased from GIBCO (Paisley, GBR).

HepaRG cells, purchased from Thermo Scientific (Wohlen, Switzerland), were cultured and differentiated as described before (Grunig *et al.*, 2017; Guillouzo *et al.*, 2007).

HepG2 cells, purchased from ATCC (Manassas, Virginia), were maintained in Dulbecco's Modified Eagle Medium (1.0 g/l glucose, 4 mM L-glutamine and 1 mM pyruvate) supplemented with 10% heat-inactivated fetal calf serum, 2 mM GlutaMAX, 10 mM 4-(2-hydroxyethyl)-1-piperazineethanesulfonic acid (HEPES) buffer, 1% MEM nonessential amino acids solution, and penicillin-streptomycin (10 000 U/ml).

*Intracellular lipid accumulation*. In order to load cells with exogenous fatty acids, cell culture media were supplemented with 1% BSA, 334 μM palmitic acid and 666 μM oleic acid. HepG2 cells were loaded with 50% fatty acid supplemented medium and HepaRG cells with 25%. After 24 h, the medium containing fatty acids was replaced by fatty acid free medium and cells exposed to toxicants for 24 h. Before FACS analysis, cells were detached using trypsin-EDTA (Thermo Scientific), washed with PBS, and then stained with 5 ng/ml BODIPY 493/503 and 10 μg/ml propidium iodide (PI) for 30 min at 37°C. After incubation, samples were kept on ice until analysis by flow cytometry.

*Fluorescence microscopy*. HepG2 and HepaRG cells were seeded in Poly-L-Lysine coated μ-Slide plates, purchased from Ibidi (Martinsried, Germany). Cells were treated with culture medium containing fatty acids (2:1 oleate:palmitate bound to BSA as described in the preceding section) followed by toxicants for 24 h, and then washed and fixed for 4 min with 4% paraformaldehyde at 37°C. After an additional washing step, cells were stained for 30 min with 0.5 μg/ml BODIPY 493/503 from Thermo Scientific and 1 μM DAPI (Thermo Scientific) in PBS at 37°C. After washing twice with PBS and the addition of antifade-mounting medium (1 mg/ml p-phenylene diamine in 90% glycerol, pH 9.2), the cells were imaged on an Olympus IX83 microscope, purchased from Olympus (Shinjuku, Japan).

*Isolation of mitochondria*. Mouse liver mitochondria were freshly isolated as originally described by Hoppel et al. for rats (Hoppel *et al.*, 1979) with the modifications described previously in Felser *et al.* (2013).

*Oxidation of 1-$^{14}$C palmitic acid, 1-$^{14}$C palmitoylcarnitine, and 1-$^{14}$C palmitoyl-CoA*. Metabolism of fatty acid oxidation substrates was assessed using permeabilized HepaRG cells and isolated mouse liver mitochondria by the methods described earlier in Felser *et al.* (2013, 2014). The reactions were started by the addition of 25 µl radioactive substrate mix, with final concentrations of 200 µM for palmitic acid, palmitoylcarnitine, or palmitoyl-CoA, containing also the radioactive substrate (0.1 pCi/assay for 1-$^{14}$C-palmitic acid, 25 pCi/assay for 1-$^{14}$C-palmitoylcarnitine, and 25 pCi/assay for 1-$^{14}$C-palmitoyl-CoA).

*Activity of long-chain acyl-CoA synthetase and carnitine palmitoyltransferase 1*. Long-chain acyl-CoA synthetase (ACSL) activity was assessed by the rate of $^{14}$C-palmitoyl-CoA formation, as described previously (Felser *et al.*, 2014).

Carnitine palmitoyltransferase (CPT) 1 activity was measured as the formation of palmitoyl-$^{14}$C-carnitine from palmitoyl-CoA and $^{14}$C-carnitine as described previously in Felser *et al.* (2014).

*Acyl-CoA dehydrogenase activities*. Activities of the respective acyl-CoA dehydrogenase isoforms were determined by the method published by Hoppel *et al.* (1979). In a 48-well plate, 50 µg of mitochondrial protein (previously frozen) was preincubated in the presence of test compounds for 5 min in the assay buffer (34 mM potassium phosphate, 1.5 mM KCN, 3.75 µM rotenone, 1.5 mM cytochrome C, 3 mM phenazine ethosulfate, pH 7.2). The reaction was started by the addition of palmitoyl-CoA or octanoyl-CoA (final concentrations 50 and 100 µM, respectively) and monitored at 550 nm over 2 min in a Tecan microplate reader (Männedorf, Switserland).

*Formation of acylcarnitines*. Acylcarnitines of interest were analyzed by liquid chromatography tandem mass spectrometry (LC-MS/MS) based on the method of Morand *et al.* (2013) with minor modifications. In brief, the supernatants of cells were mixed with internal standard solution, containing deuterated standards in methanol, in a ratio of 1:3 (v/v). The mixtures were centrifuged before they were transferred to an autosampler tube and diluted 1:1 with water. For analysis we used a LC-MS/MS system consisting of a Nexera SIL-30AC autosampler, a column-oven (CTO-20A), 4 HPLC pumps (2× LC-20AD and 2× LC-ADXR) and a system controller (CBM-20A), all acquired from Shimadzu (Kyoto, Japan). The HPLC system was coupled to an API 4000 triple quadrupole mass spectrometer from AB Sciex (Concord, California), equipped with a turbo electrospray ionization source.

For sample separation a Luna C8 5 µM column (150 × 2 mm) was used at 50°C. Reference substances were obtained for acetylcarnitine, octanoylcarnitine, and palmitoylcarnitine and used as standards and for quality control.

*Western blotting*. After 24 h of incubation with the drugs, the cells were washed with PBS and lysed with RIPA buffer (50 nM Tris-HCL, pH 7.4, 150 mM NaCl, 1% Triton X-100, 0.5% sodium deoxycholate, 0.1% sodium dodecylsulfate, and 1 mM EDTA in water), containing 1 tablet of complete Mini Protease inhibitor cocktail from Roche Diagnostics (Rotkreuz, Switzerland) per 10 ml of buffer. Lysates were incubated with RIPA buffer under constant agitation for 15 min and then centrifuged at 15 700 × g for 10 min at 4°C. After determining the protein content with Pierce BCA Protein Assay Kit (Thermo Scientific) 15 µg of protein was separated on 4%–12% bis-tris gradient gel (Invitrogen, Carlsbad, California), and transferred to polyvinylidene difluoride membranes, using the Trans-Blot Turbo Transfer System (Bio-Rad, Hercules, Califronia). All primary antibodies were obtained from Abcam (Cambridge, UK) and diluted 1:1000. Exceptions were antibodies against adipose differentiation-related protein (ADRP) and glyceraldehyde 3-phosphate dehydrogenase (GAPDH), which were obtained from Santa Cruz Biotechnology and diluted 1:250 and 1:5000, respectively, as well as ACSL1 antibody, which was obtained from Cell Signaling Technology (Danvers) and diluted 1:1000. The secondary antibodies were from Santa Cruz Biotechnology and used at a dilution of 1:2000. Protein bands were normalized to GPDH.

*mRNA quantification*. For RNA extraction and purification, the Qiagen RNeasy Mini Extraction Kit (Qiagen, Hilden, Germany) was used and for RNA quality evaluation a NanoDrop 2000 (Thermo Scientific) was used. cDNA was synthesized from 1 µg RNA, using the Qiagen Omniscript system. mRNA quantification was conducted using FastStart Universal SYBR Green Master from Roche in a ViiA 7 Real Time PCR System from Applied Biosystems (Waltham, Massachusetts). The relative quantity of specifically amplified cDNA was calculated by the comparative-threshold cycle method. As endogenous reference, GAPDH was used and no-template and no-reverse-transcription controls ensured the absence of nonspecific amplification. The specific primers used are given in Supplementary Table 1.

*Hepatocellular export of ApoB100*. Levels of ApoB100 in the supernatants of the cells were measured in order to assess the excretion of triglycerides. The ApoB Quantikine ELISA Kit from R&D Systems (Minneapolis, Minnesota) was used according to the manufacturer's protocol with some modifications. For that, 145 µl assay diluent RD1-113 plus 5 µl calibrator diluent RD-61 were added to each well before the addition of 100 µl cell supernatant.

*Statistical analysis*. Data are given as the mean ± SEM of at least 3 independent experiments. Statistical analyses were performed using GraphPad Prism 6 (GraphPad Software, La Jolla, California). For the comparison of treatment groups to the 0.1% DMSO control group, 1-way ANOVA was used followed by the Dunnett's posttest procedure. The $p$-values $< .05$ (*) were considered significant.

## RESULTS

### *Intracellular Lipid Accumulation*

We first investigated the potential of tolcapone and entacapone for cellular neutral lipid accumulation using the dye BODIPY 493/503 and flow cytometric analysis in HepaRG and in HepG2 cells. Both HepaRG cells (Figure 1B) as well as HepG2 cells (Figure 1C) treated with tolcapone for 24 h showed a concentration-dependent increase in intracellular lipid content. For tolcapone, this increase started at 50 µM and reached statistical significance at 100 and 200 µM in both cell types. In comparison, entacapone caused a significant accumulation of lipids only in HepG2 (200 µM), but not in HepaRG cells. TC, an efficient inhibitor of fatty acid activation (Igal *et al.*, 1997), did not affect lipid accumulation in HepaRG cells (Figure 1B) and decreased lipid accumulation in HepG2 cells (Figure 1C).

The results obtained by flow cytometry were qualitatively confirmed using fluorescence microscopy (Figure 1D for HepaRG and Supplementary Figure 2 for HepG2 cells). Both cell lines showed accumulation of small lipid droplets in green

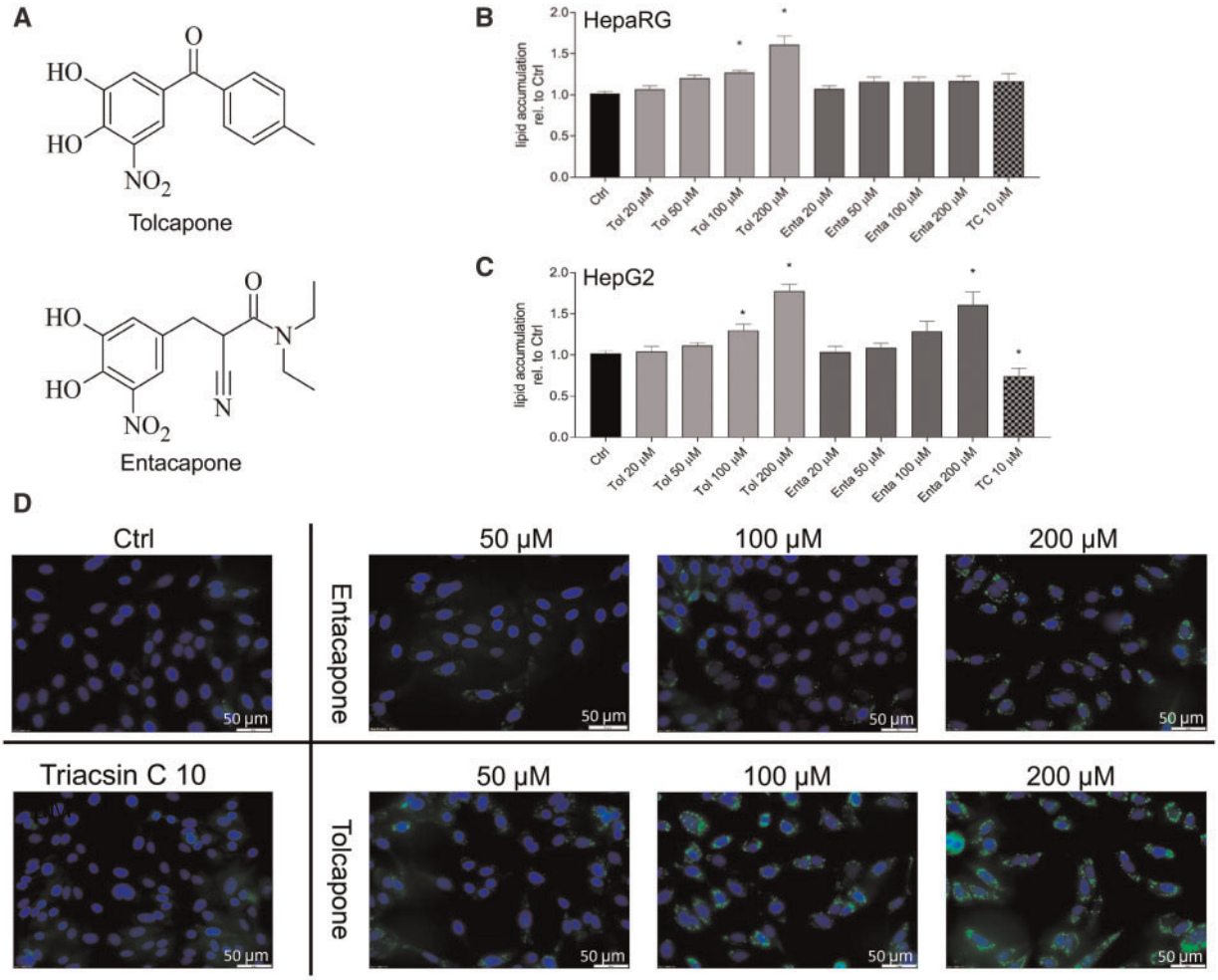


**Figure 1.** Effect on intracellular lipid accumulation in HepaRG cells. Cells were first cultured for 24 h in a medium containing BSA-bound palmitate and oleate before treatment with the compounds of interest. A, Chemical structure of tolcapone and entacapone. B, Fold change in lipid accumulation in HepaRG cells. After treatment with the compounds of interest for 24 h, cells were stained with PI and BODIPY493/503 and analyzed by FACS. Results are presented as mean ± SEM of 6 independent experiments. $^*p < .05$ versus DMSO 0.1% control. C, Fold change in lipid accumulation in treated HepG2 cells. HepG2 cells were treated and analyzed as described for HepaRG cells. Results are presented as mean ± SEM of 6 independent experiments. $^*p < .05$ versus DMSO 0.1% control. D, Representative fluorescence microscopy pictures of HepaRG cells treated with the compounds of interest for 24 h. After treatment, cells were stained with PI for nuclei and BODIPY493/503 for neutral lipids.

around the nucleus in blue when treated with tolcapone. Similar to the flow cytometric analysis, also entacapone (200 µM) produced an increased number of lipid droplets in HepG2 cells, but, in contrast to cytometry, also in HepaRG cells. Treatment with TC led to a decrease of triglyceride incorporation into lipid droplets in both cell lines, as suggested by dissemination of a faint BODIPY signal throughout the cells with very small lipid droplets.

### *Cellular Fatty Acid Metabolism* In Vitro

To elucidate the mechanism leading to lipid accumulation, we assessed the metabolism of various fatty acid oxidation substrates in HepaRG cells treated for 24 h. We could observe a decrease in β-oxidation capacity of palmitate (Figure 2A) after treatment with tolcapone starting at 100 µM but not entacapone. CPT1 activity (Figure 2B), which is considered the rate-limiting step in lipid oxidation (Bonnefont *et al.*, 2004), was not affected by tolcapone or entacapone treatment. Moreover, the metabolism of palmitoyl-CoA was unchanged (Figure 2C), indicating that transport of fatty acids into mitochondria and mitochondrial β-oxidation were not affected. These findings suggested an inhibition of fatty acid metabolism by tolcapone before entry into mitochondria, pointing towards an effect on fatty acid activation (synthesis of acyl-CoAs). This was confirmed directly for tolcapone, which inhibited activation of palmitate starting at 50 µM (Figure 2D). In contrast, entacapone did not inhibit palmitate activation in HepaRG cells.

### *Mitochondrial Fatty Acid Metabolism*

Next, we determined the inhibitory capability of the drugs on freshly isolated mouse liver mitochondria. Similar to the findings in HepaRG cells, we observed inhibition of palmitate metabolism by tolcapone (Supplementary Figure 2A), but starting at lower concentrations (at 5 µM) compared with HepaRG cells (where inhibition started at 100 µM, see Figure 2A). Interestingly, also entacapone-inhibited palmitate metabolism in isolated mouse liver mitochondria, starting at 50 µM. As we had observed already in HepaRG cells, metabolism of palmitoylcarnitine (Supplementary Figure 3B) and palmitoyl-CoA (Supplementary Figure 3C) was affected neither by tolcapone,

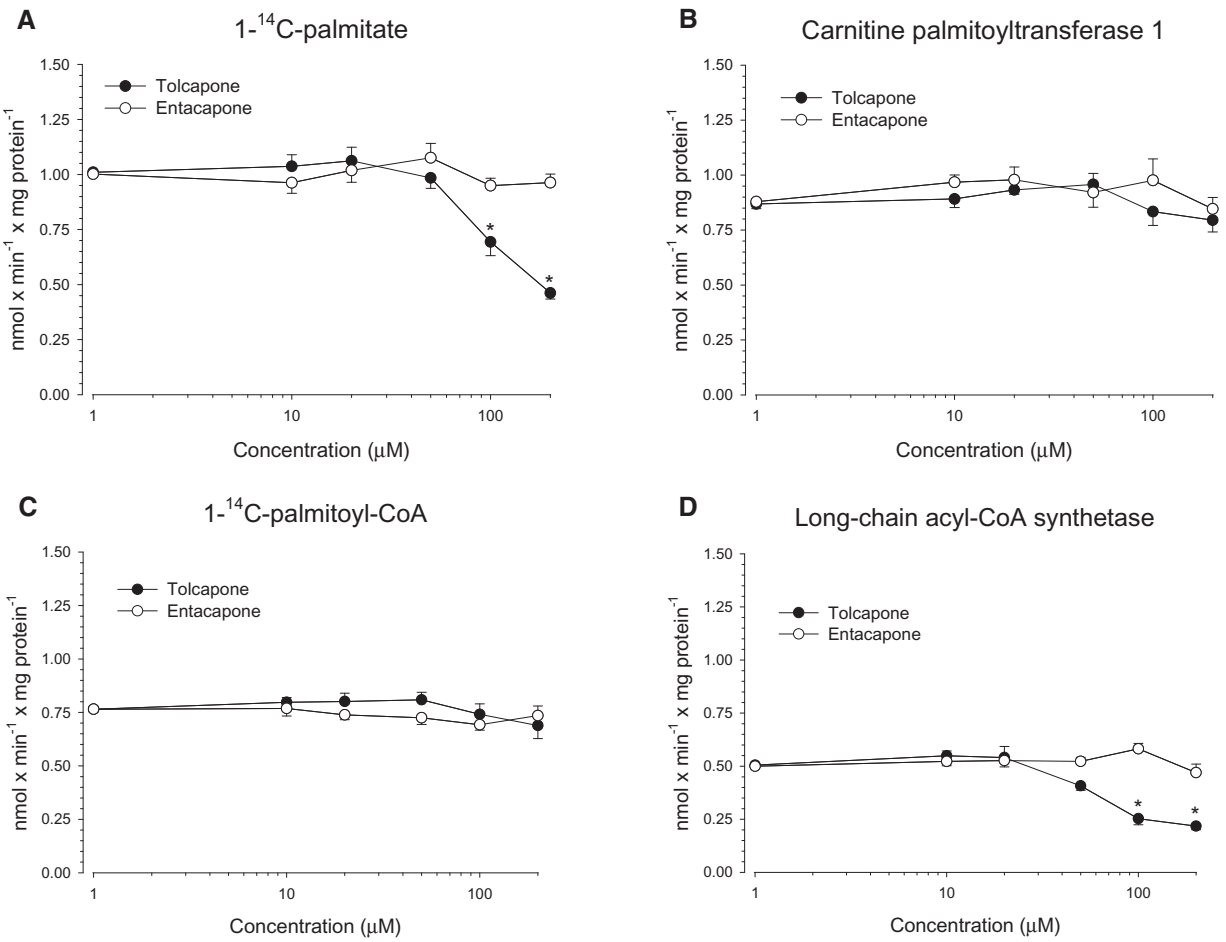


**Figure 2.** Effect of tolcapone and entacapone on fatty acid metabolism in HepaRG cells. Cells were treated with the compounds of interest for 24 h, before determining (A) metabolism of $^{14}$C-palmitic acid (control activity 0.98 ± 0.06 nmol × min$^{-1}$ × mg protein$^{-1}$), (B) activity of CPT1 (control activity 0.82 ± 0.06 nmol × min$^{-1}$ × mg protein$^{-1}$), (C) metabolism of 1-$^{14}$C-palmitoyl-CoA (control activity 0.75 ± 0.05 nmol × min$^{-1}$ × mg protein$^{-1}$) and (D) activity of ACSL (control activity 0.51 ± 0.03 nmol × min$^{-1}$ × mg protein$^{-1}$). Results are presented as mean ± SEM of at least 8 independent experiments. *$p < .05$ versus DMSO 0.1% control.

nor by entacapone. Similar to HepaRG cells, inhibition of palmitate activation (synthesis of palmitoyl-CoA) by tolcapone was also detectable for isolated mitochondria (Supplementary Figure 3D), while entacapone did not affect palmitate activation under these conditions.

### *Changes in Acylcarnitine Pattern*

As published recently, the pattern of acylcarnitines excreted by cells can be useful for the detection of specific inhibitions in fatty acid metabolism (Grünig *et al.*, 2018). Treatment with tolcapone was associated with a concentration-dependent decrease in medium-chain acylcarnitine formation (C5 to C10 acylcarnitines; starting at 50 µM) with a concomitant increase in 3-oxo-palmitoylcarnitine (starting at 50 µM) and an increase in C12–C16 acylcarnitines at higher concentrations (starting at 100 µM) (Figure 3A). In comparison, entacapone treated HepaRG cells showed a similar, but less pronounced depression of medium-chain acylcarnitine formation (Figure 3B), starting at 100 µM. Moreover, the effects on long-chain-acylcarnitines (C14 and C16) and 3-oxo-palmitoylcarnitine were less pronounced compared with tolcapone.

For the purpose of pattern comparison and proof of concept, we also studied the effect of the acyl-CoA synthesis inhibitor TC (Igal *et al.*, 1997), the CPT1 inhibitor etomoxir (Ceccarelli *et al.*, 2011), the medium-chain acyl-CoA dehydrogenase inhibitor methylenecyclopropyl acetic acid (MCPA) (Tserng *et al.*, 1991), and the 3-keto-acyl-CoA thiolase inhibitor 4-bromocrotonic acid (Olowe and Schulz, 1982) on the acylcarnitine pattern in the supernatant of HepaRG cells. As shown in Figure 3C, the established inhibitors affected the acylcarnitine pattern in predictable fashion. TC and etomoxir decreased all acylcarnitines determined, showing the importance of fatty acid activation and acylcarnitine formation for mitochondrial hepatocellular long-chain fatty acid metabolism. MCPA was associated with an increase in the medium-chain acylcarnitines, demonstrating the block of medium-chain acyl-CoA dehydrogenase and 4-bromocrotonic acid with the expected increase in 3-oxo-palmitoylcarnitine.

### *Activity of Acyl-CoA Dehydrogenases*

Because of the increase in excreted long-chain acylcarnitines after tolcapone treatment (Figure 3A), we determined the effect of tolcapone and entacapone on the activity of acyl-CoA dehydrogenases in liver mitochondria. Tolcapone showed a concentration-dependent decrease in the activity of the long-chain acyl-CoA dehydrogenase, reaching statistical significance at the highest concentration investigated (400 µM). In contrast, tolcapone did not affect medium-chain acyl-CoA dehydrogenase (Supplementary Figure3B) and entacapone did affect the

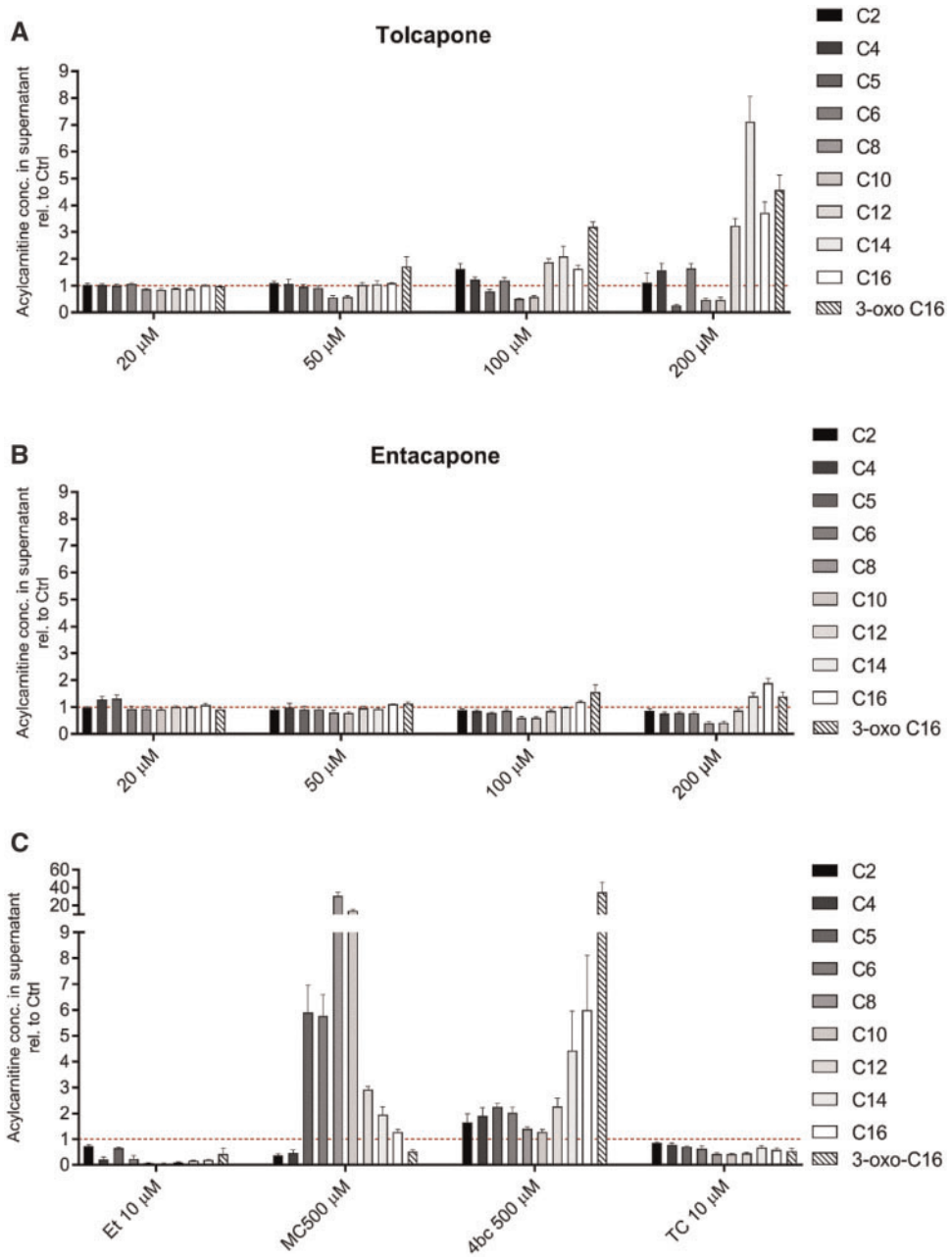


**Figure 3.** Effect of tolcapone, entacapone, TC, etomoxir, methylenecyclopropaneacetic acid, and 4-bromocrotonic acid on the acylcarnitine pattern in the supernatant of HepaRG cells. HepaRG cells were treated with the toxicants for 24 h in the presence of oleate, palmitate and L-carnitine. The supernatant was analyzed using LC-MS/MS as described in the Methods section. Results were normalized to the values of DMSO 0.1% exposed control cells and are expressed as mean ± SEM of 3 independent experiments. Abbreviations: TC, triacsin C; Et, etomoxir; MC, methylene-cyclopropane acetic acid; 4bc, 4-bromocrotonic acid.

activity of neither long- nor medium-chain acyl-CoA dehydrogenase (Supplementary Figs. 3A and 3B).

### *Effects on mRNA and Protein Expression of ACSL*

To elucidate potential mechanisms how tolcapone could inhibit palmitate activation, we investigated mRNA and protein expression ACSL1 and ACSL5, which are considered to be associated with mitochondria (Soupene and Kuypers, 2008).

As shown in Figures 4A and 4B, tolcapone decreased mRNA expression of ACSL1 starting at 100 µM, but had no significant effect on ACSL5 mRNA expression. In comparison, entacapone and TC did not affect mRNA expression of ACSL1 and ACSL5. As shown in Figures 4C and 4D, and Supplementary Figure 4, tolcapone decreased protein expression of ACSL1 and 5 at the highest concentration investigated (200 µM), whereas entacapone and TC did not affect protein expression of ACSL1 and 5.

### *Effects on Markers of Fatty Acid Import, Synthesis and Trafficking, Lipid Storage, and Lipid Excretion*

Hepatocytes can maintain their fatty acid pool by import and by de novo synthesis. As shown in Figures 5A and 5B, tolcapone was associated with a significant increase in the mRNA expression of CD36/FAT and with a numerical increase in the mRNA expression of fatty acid transport protein 5 (FATP5), 2 proteins

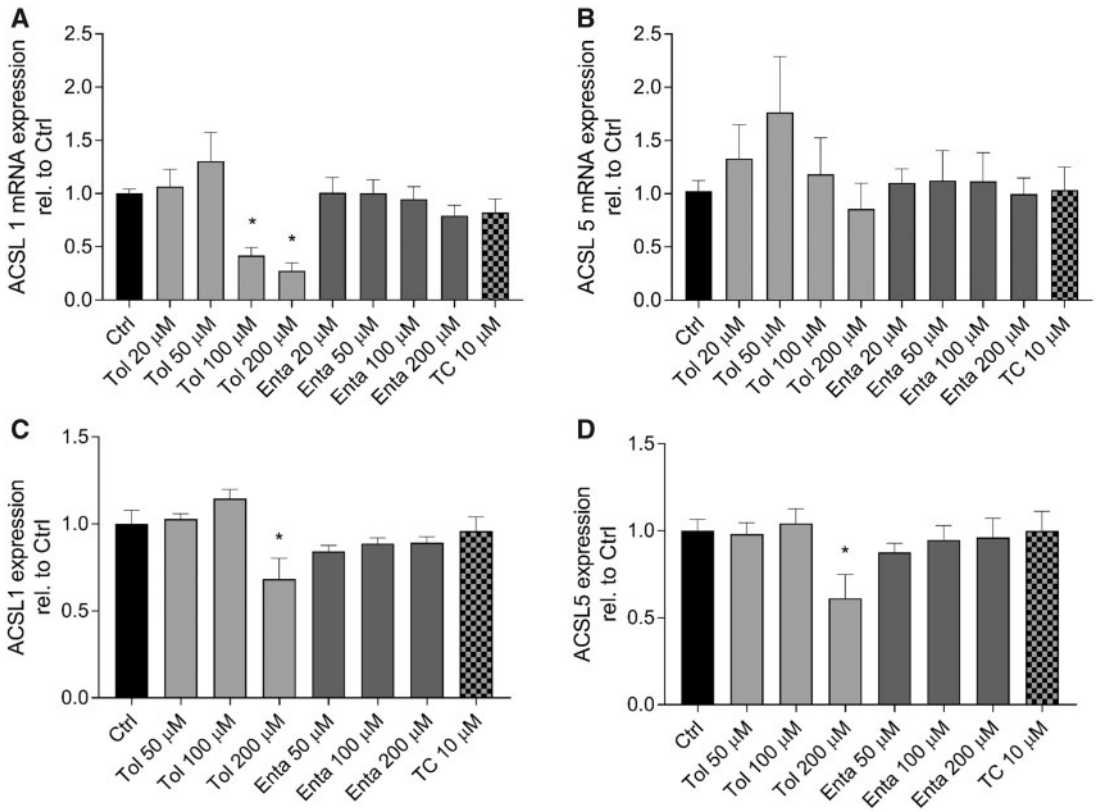


**Figure 4.** Effect of tolcapone and entacapone on mRNA and protein expression of ACSLs in HepaRG cells. Cells were treated for 24 h with the drugs before determination of mRNA and protein content of ACSL. A, Fold change in mRNA expression of ACSL1 and (B) fold change in mRNA expression of ACSL5. C, Quantification of a Western blot showing fold change in ACSL1 expression and (D) fold change in ACSL5 expression. Results are normalized to control cells exposed to 0.1% DMSO and are presented as mean ± SEM of 4 independent experiments. $^*p < .05$ versus DMSO 0.1% control. Abbreviations: Ctrl, control (DMSO 0.1%); Tol, tolcapone; Enta, entacapone; TC, triacsin C.

involved in fatty acid import (Bechmann *et al.*, 2012; Kazantzis and Stahl, 2012). In comparison, entacapone did not affect mRNA expression of CD36/FAT (Figure 5A) and decreased FATP5 mRNA expression (Figure 5B). As shown in Figure 5C and Supplementary Figure 4, the liver fatty acid-binding protein (FABP), which is important for intracellular binding and transport of fatty acids and intermediates (Wang *et al.*, 2015), was not significantly affected by tolcapone, entacapone or TC.

Tolcapone reduced mRNA expression of the sterol regulatory element-binding protein-1c (SREBP-1c), which is a regulator of fatty acid synthesis (Eberle *et al.*, 2004) (Figure 5D). Accordingly, tolcapone reduced also the mRNA expression of acetyl-CoA carboxylase (ACC, Figure 5E) and fatty acid synthase (FAS, Figure 5F), which encode 2 essential proteins in fatty acid synthesis (Bechmann *et al.*, 2012). In comparison, entacapone and triacsin did not affect the mRNA expression of the corresponding genes.

Next, we investigated triglyceride synthesis and lipid droplet formation. The protein expression of glycerol-3-phosphate acyltransferase 1 (GPAT1), which catalyzes the first step in glycerolipid (eg, triglyceride) synthesis (Wendel *et al.*, 2009), was not affected by tolcapone or TC, whereas entacapone decreased the expression of GPAT1 concentration-dependently, reaching statistical significance at 200 µM (Figure 6A and Supplementary Figure 4).

Protein expression of perilipin-2, also known as ADRP, which is involved in lipid droplet formation (Brasaemle *et al.*, 1997), was not affected by entacapone or TC (Figure 6B and Supplementary Figure 4), whereas tolcapone numerically decreased ADRP protein expression at 200 µM. In contrast, mRNA expression of the cell death-inducing DNA fragmentation factor-alpha-like effector a (cidea), encoding a protein involved in lipid droplet formation (Zhou *et al.*, 2012), was significantly increased by tolcapone (100 µM) (Figure 6C). In comparison, entacapone and triacsin did not affect cidea mRNA expression.

The protein content of the microsomal triglyceride transfer protein (MTTP), which is essential for lipidation of ApoB100 (Mason, 1998), was not affected by entacapone or TC (Figure 6D and Supplementary Figure 4). In comparison, tolcapone increased the protein expression of MTTP concentration-dependently, reaching statistical significance at 200 µM.

Hepatocytes can export triglycerides in the form of VLDL. Since ApoB100 is the protein core of VLDL, we determined the ApoB concentration in the supernatant of HepaRG cells exposed to the toxicants. Treatment with tolcapone was associated with a concentration-dependent decrease in the ApoB100 concentration, reaching statistical significance at 100 µM (Figure 6E), whereas entacapone and TC did not significantly affect ApoB100 secretion. As shown in Figure 6F, tolcapone decreased mRNA expression of ApoB starting at 100 µM, suggesting that impaired transcription of the ApoB100 gene could be the reason for the observed decrease in ApoB100 secretion. Entacapone did not affect ApoB100 secretion or mRNA expression, whereas TC increased ApoB100 mRNA expression without affecting ApoB100 secretion (Figs. 6E and 6F).

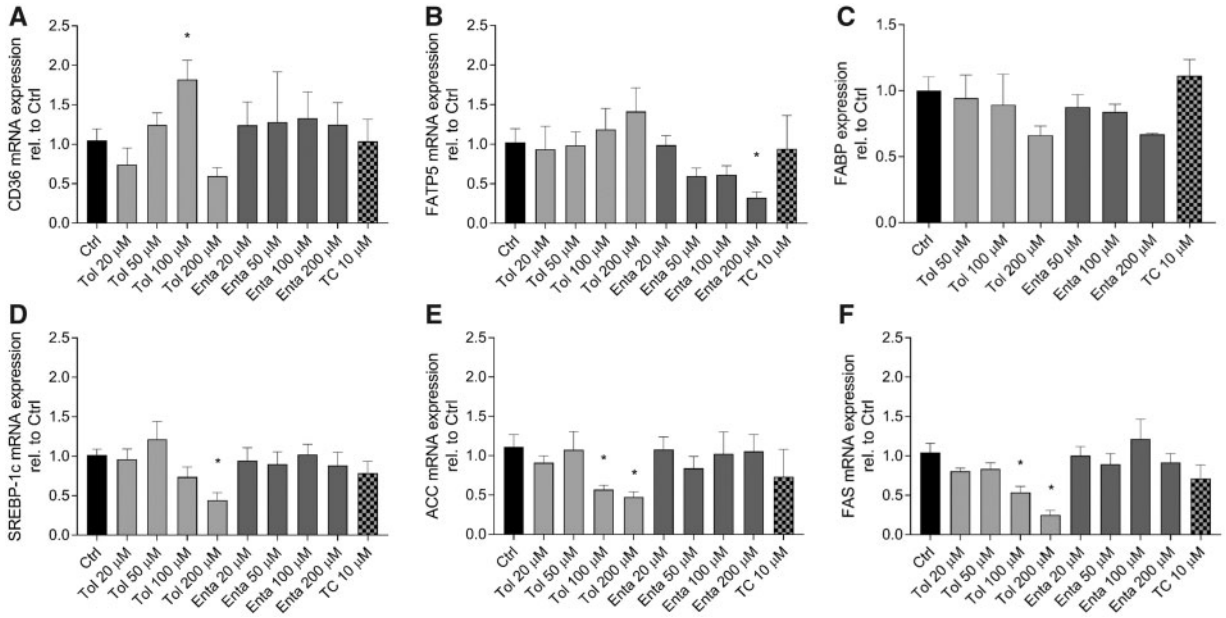


Figure 5. Effect of tolcapone and entacapone on mRNA or protein expression of fatty acid transporters, transport proteins and proteins involved in fatty acid synthesis in HepaRG cells. Cells were treated for 24 h with the drugs before determination of the mRNA or protein content. A, Fold change in mRNA expression of CD36/FAT, (B) fold change in mRNA expression of FATP5, (C) fold change in the protein content of FABP, (D) fold change in mRNA expression of SREBP-1c, (E) fold change in mRNA expression of ACC, and (F) fold change in FAS mRNA expression. Results are normalized to control cells exposed to 0.1% DMSO and are presented as mean ± SEM of 4 independent experiments. *$p < .05$ versus DMSO 0.1% control. Abbreviations: Ctrl, control (DMSO 0.1%); Tol, tolcapone; Enta, entacapone; TC, triacsin C; FATP, fatty acid transport protein; FABP, fatty acid-binding protein; SREBP, sterol regulatory element-binding protein; ACC, acetyl-CoA carboxylase; FAS, fatty acid synthase.

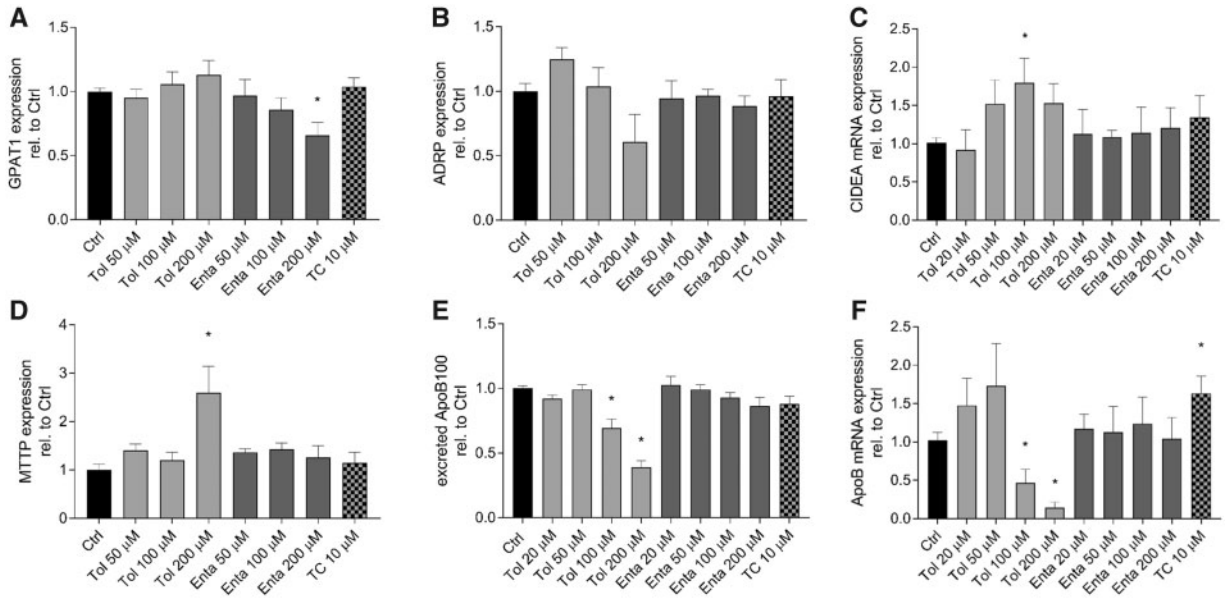


Figure 6. Effect of tolcapone and entacapone on mRNA or protein expression of proteins involved in triglyceride synthesis, lipid droplet formation or VLDL formation and export in HepaRG cells. Cells were treated for 24 h with the drugs before determination of the mRNA or protein content. A, Fold change in GPAT1 protein expression. B, Fold change in ADRP protein expression. C, Fold change in cidea mRNA expression. D, Fold change in MTTP protein expression. E, Fold change in ApoB100 protein excreted into the supernatant of HepaRG cell cultures. The mean concentration of ApoB100 in the supernatant of control cells (exposed to 0.1% DMSO) was 26.2 ± 1.3 ng × $mL^{-1}$. F, Fold change in mRNA ApoB100 expression. Results were normalized to control incubations exposed to 0.1% DMSO and are presented as mean ± SEM of $n = 5$ independent experiments. *$p < .05$ versus DMSO 0.1% control. Abbreviations: Ctrl, control (DMSO 0.1%); Tol, tolcapone; Enta, entacapone; TC, triacsin C; GPAT, glycerol-3-phosphate acyltransferase; ADRP, adipose differentiation-related protein; cidea, cell death-inducing DNA fragmentation factor-alpha-like effector a; MTTP, microsomal triglyceride transfer protein; ApoB, apolipoprotein B.

## DISCUSSION

This study illustrates that tolcapone is associated with lipid accumulation in HepaRG and HepG2 cells, which, as shown HepaRG cells, can be explained by increased fatty acid import, impaired mitochondrial fatty acid metabolism and impaired secretion of VLDL.

After having entered the hepatocytes, fatty acids are activated and can subsequently undergo degradation by

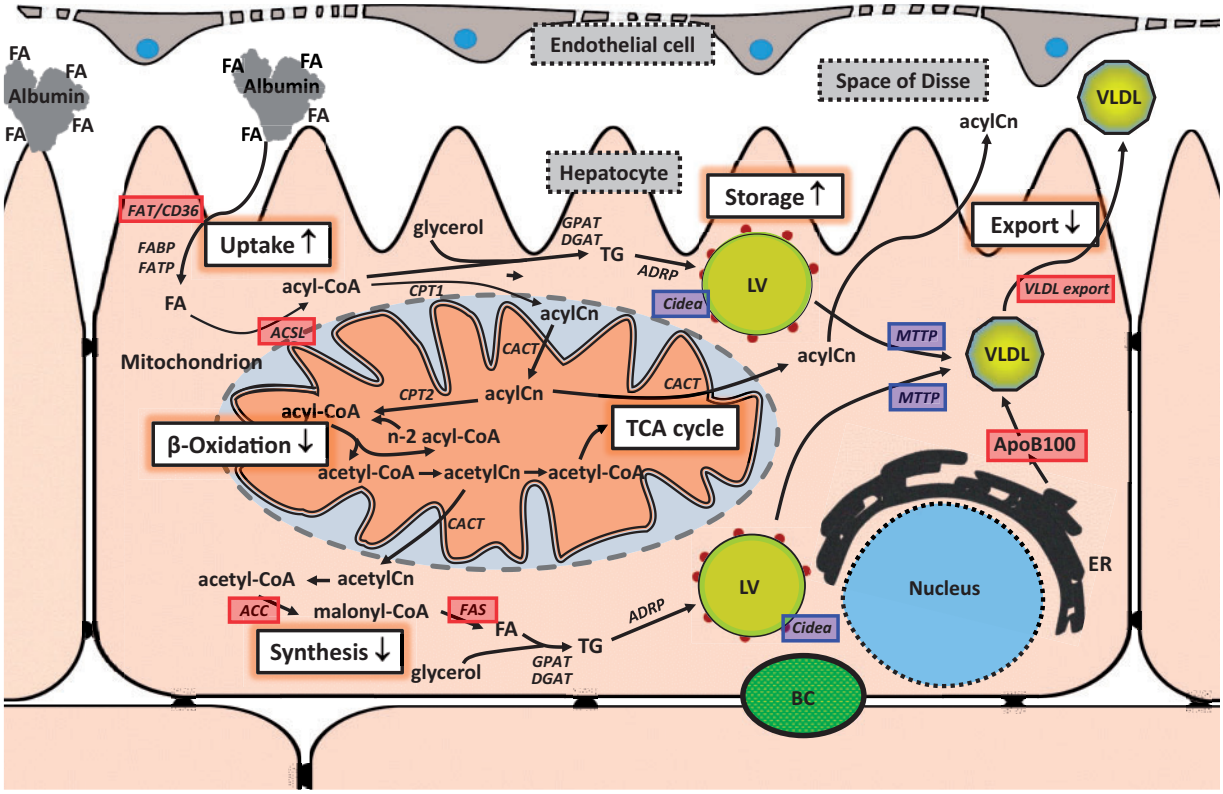


**Figure 7.** Hepatocellular fatty acid metabolism. Long-chain fatty acids (FA) are imported into hepatocytes by mainly active transport and diffusion (Uptake). Subsequently, they can be activated to the corresponding CoA derivative by ACSLs. The activated fatty can be converted to the carnitine (Cn) derivative by CPT1, imported into the mitochondrial matrix by COCT and reconverted to the corresponding CoA derivative by CPT2. This is followed by β-oxidation, which produces acetyl-CoA, NADH, and $FADH_2$ (not shown). Acyl-CoAs can be converted to the corresponding carnitine derivatives, which can be exported from mitochondria (and cells) by COCT. Hepatocytes can also synthesize fatty acids starting from malonyl-CoA (Synthesis), which is regulated by SREBP-1c (not shown). Depending on the metabolic conditions, activated fatty acids can also be used for triglyceride (TG) synthesis. Triglycerides can be stored in lipid vesicles (LV) (Storage). ADRP and cidea are 2 proteins involved in lipid droplet formation. Triglycerides can also be used for the synthesis of VLDL, which can be exported (Export). Effects of tolcapone are indicated with arrows and with red (decrease) or blue boxes (increase) around critical proteins or activities. Abbreviations: ACC, acetyl-CoA carboxylase; ACSL, long-chain acyl-CoA synthetase; ADRP, adipose differentiation-related protein; ApoB, apolipoprotein B; BC, bile canaliculus; CACT, carnitine-acylcarnitine translocase; cidea, cell death-inducing DNA fragmentation factor-alpha-like effector a; CPT, carnitine palmitoyltransferase; DGAT, diacylglycerol-O-acyltransferase; ER, endoplasmic reticulum; FA, long-chain fatty acids; FABP, fatty acid binding protein; GPAT, glycerol-3-phosphate acyltransferase; LV, lipid vesicle; MTTP, microsomal triglyceride transfer protein; SREBP-1c, sterol regulatory element-binding protein 1c; VLDL, very low-density lipoprotein.

β-oxidation or can be used for triglyceride production. Triglycerides can be stored in lipid droplets or can be incorporated into VLDL particles that are exported from hepatocytes (Figure 7). In order to find out possible reasons why tolcapone is associated with lipid accumulation in hepatocytes, we assessed these pathways using different approaches. First, we confirmed that tolcapone (and less so entacapone) is associated with hepatocellular lipid accumulation. For that we chose 2 frequently used cell models, HepG2 cells and the better differentiated HepaRG cells (Berger *et al.*, 2016). In both cell models, tolcapone was associated with lipid accumulation starting at 100 μM, whereas entacapone reached a significant accumulation only in HepG2 cells at 200 μM. Although better differentiated, HepaRG cells seem to be slightly less sensitive to inhibition of fatty acid metabolism than HepG2 cells. The suitability of HepG2 cells for studying fatty acid metabolism has been demonstrated previously in Donato *et al.* (2009) and Felser *et al.* (2013). Nevertheless, since we wanted to study the mechanisms and not the extent of lipid accumulation, we chose the better differentiated HepaRG cells for our investigations.

The mRNA expression of CD36/FAT and FATP5 was concentration-dependently increased by tolcapone, indicating an augmentation in transcription and possibly also in protein expression and activity of these transporters. These findings offered 1 possible explanation for the observed lipid droplet accumulation by tolcapone in HepaRG cells.

Considering the description of microvesicular steatosis in a patient with tolcapone-associated liver injury (Spahr *et al.*, 2000), impairment of mitochondrial fatty acid metabolism could be expected (Fromenty and Pessayre, 1995). Furthermore, we and others have reported that tolcapone impairs the function of the mitochondrial electron transport chain (Grunig *et al.*, 2017; Haasio *et al.*, 2002a), which can disturb mitochondrial fatty acid metabolism. In agreement with these reports, palmitate metabolism was reduced in HepaRG cells and in acutely exposed isolated mouse liver mitochondria. To our surprise, however, β-oxidation (metabolism of palmitoylcarnitine and palmitoyl-CoA) was intact and we could localize the defect in mitochondrial fatty acid metabolism in the activation of long-chain fatty acids. There are several acyl-CoA synthases performing activation of fatty acids, depending on the chain-length of the fatty acids to be activated and with different subcellular localization (Soupene and Kuypers, 2008). ACSLs localized on the outer mitochondrial membrane, which are responsible for the activation

of long-chain fatty acids undergoing mitochondrial metabolism, are mainly ACSL1 and ACSL5 (Soupene and Kuypers, 2008). Based on our findings, we can propose 2 mechanisms how tolcapone affects the mitochondrial ACSLs. The data in isolated mitochondria indicate an acute inhibition, which is most probably the result of a direct interaction of tolcapone with the mitochondrial ACSLs. The second mechanism was detected in HepaRG cells exposed for 24 h. In these experiments, we observed a decrease in the mRNA and protein expression of mainly ACSL1, the most active ACSL in liver (Yan *et al.*, 2015), suggesting an inhibition of the transcription of the gene encoding ACSL1.

TC, which was used as a positive control, is an inhibitor of ACSL1, ACSL3, and ACSL4 (Tomoda *et al.*, 1991). In contrast to tolcapone, TC was not associated with hepatocellular accumulation of lipids (Figure 1). This difference compared with tolcapone may be explained by inhibition of nonmitochondrial ACSLs, which are important for triglyceride synthesis (Soupene and Kuypers, 2008).

We determined the acylcarnitine pool in the HepaRG culture supernatant as an additional marker of mitochondrial fatty acid metabolism (see Figure 7). We have shown previously that the acylcarnitine pool in cell culture supernatant can be used for localizing defects in mitochondrial fatty acid metabolism (Grünig *et al.*, 2018). Acylcarnitines are formed from the respective acyl-CoAs by carnitine acyltransferases (Brass and Hoppel, 1980) and can be transported out of mitochondria and cells into the circulation (Vernez *et al.*, 2003) or into cell culture supernatants. The acylcarnitine pattern in cell culture supernatants describes therefore the cellular (and mitochondrial) acyl-CoA pattern, which can reflect alterations in fatty acid metabolism (Ensenauer *et al.*, 2012). In this study, treatment of HepaRG cells was associated with a decrease in medium-chain acylcarnitines starting at 50 μM and an increase in long-chain acylcarnitines starting at 100 μM. The decrease in medium-chain acylcarnitines was less accentuated as observed with TC, but can be explained by inhibition of fatty acid activation. The concomitant increase in the long-chain acylcarnitines, which occurred at higher concentrations, can be explained by the observed inhibition of the long-chain acyl-CoA dehydrogenase. The results of the acylcarnitine pattern are therefore in agreement with the findings obtained with direct determination of enzyme activities.

A third mechanism for the observed increase in lipid droplet accumulation in HepaRG cells treated with tolcapone was an impaired export of VLDL (and therefore triglycerides) out of hepatocytes as suggested by impaired ApoB100 excretion (see Figure 7). Every LDL particle contains 1 ApoB100 molecule, which is the structural protein of the LDL particle and essential for VLDL formation (Fisher, 2012; Mason, 1998). We also observed reduced ApoB100 mRNA levels in HepaRG cells treated with tolcapone, suggesting that the reason for reduced ApoB100 in tolcapone-treated cells may be impaired ApoB100 synthesis. In addition, degradation of ApoB100 has been reported to be important for the cellular ApoB100 levels and to involve ApoB100 oxidation followed by autophagy (Fisher, 2012). Since tolcapone was associated with mitochondrial ROS production (Grunig *et al.*, 2017), ApoB100 degradation could be increased in the presence of tolcapone. Since the protein expression of important factors in FABP, triglyceride synthesis (GPAT1), lipid droplet formation (ADRP), and MTTP were either not significantly affected or increased by tolcapone, lipid trafficking and lipid loading of ApoB100 appear not the be the principle reasons for impaired VLDL secretion by tolcapone-treated HepaRG cells.

In isolated mouse liver mitochondria, we observed a decrease in palmitate metabolism at 5 μM for tolcapone and at 50 μM for entacapone. In HepaRG cells, long-chain fatty acid metabolism (based on the acylcarnitine pattern in the cell culture supernatant) started to be disturbed at a tolcapone concentration of 50 μM, whereas most other alterations in fatty acid metabolism started at 100 μM. Similar concentrations were also needed to disturb the function of the mitochondrial respiratory chain of HepaRG cells in a previous study (Grunig *et al.*, 2017). The difference between mitochondria and HepaRG cells is most likely a consequence of better accessibility of mitochondria and lack of protein in the incubations with mitochondria. A recent in silico study suggested that both hepatic exposure and preexisting mitochondrial dysfunction are the key factors determining the occurrence of liver injury in patients treated with tolcapone (Longo *et al.*, 2016). The estimated liver concentrations that can be reached with therapeutic doses of tolcapone were 1–3 and 0.3–1.3 μM for entacapone. In comparison, maximal plasma concentrations reached after single doses of 200-mg entacapone (6 μM) and 100-mg tolcapone (17 μM) were higher (Kaakkola, 2000), but still lower than the lowest concentrations associated with toxicity in HepaRG cells. A suitable explanation for severe hepatic toxicity in patients treated with tolcapone is therefore that such patients must have high hepatic exposures and a preexisting mitochondrial disease. This concept has been illustrated recently in an *in vitro* study investigating the toxicity of different mitochondrial toxicants in HepG2 cells (Haegler *et al.*, 2015) and explains the infrequence of severe hepatotoxicity in patients treated with tolcapone. For entacapone, exposures reached and mitochondrial toxicity are not pronounced enough to result in liver toxicity.

In conclusion, tolcapone increases mRNA expression of fatty acid transporting proteins, inhibits activation of long-chain fatty acids and impairs VLDL secretion by hepatocytes, leading to hepatocellular triglyceride accumulation. Entacapone exhibits similar toxic effects than olcapone but at higher concentrations.

## SUPPLEMENTARY DATA

Supplementary data are available at *Toxicological Sciences* online.

## FUNDING

This study was supported by a grant from the Swiss National Science Foundation to S.K. (SNF 31003A-132992).

## REFERENCES

Assal, F., Spahr, L., Hadengue, A., Rubbici-Brandt, L., and Burkhard, P. R. (1998). Tolcapone and fulminant hepatitis. *Lancet* **352**, 958.

Bechmann, L. P., Hannivoort, R. A., Gerken, G., Hotamisligil, G. S., Trauner, M., and Canbay, A. (2012). The interaction of hepatic lipid and glucose metabolism in liver diseases. *J. Hepatol.* **56**, 952–964.

Berger, B., Donzelli, M., Maseneni, S., Boess, F., Roth, A., Krahenbuhl, S., and Haschke, M. (2016). Comparison of Liver Cell Models Using the Basel Phenotyping Cocktail. *Front. Pharmacol.* **7**, 443–410. 3389/fphar.2016.00443.

Bonnefont, J. P., Djouadi, F., Prip-Buus, C., Gobin, S., Munnich, A., and Bastin, J. (2004). Carnitine palmitoyltransferases 1 and 2:

Biochemical, molecular and medical aspects. *Mol. Aspects Med.* **25**, 495–520.

Borges, N. (2003). Tolcapone-related liver dysfunction: Implications for use in Parkinson's disease therapy. *Drug Saf.* **26**, 743–747.

Brasaemle, D. L., Barber, T., Wolins, N. E., Serrero, G., Blanchette-Mackie, E. J., and Londos, C. (1997). Adipose differentiation-related protein is an ubiquitously expressed lipid storage droplet-associated protein. *J. Lipid Res.* **38**, 2249–2263.

Brass, E. P., and Hoppel, C. L. (1980). Relationship between acid-soluble carnitine and coenzyme A pools in vivo. *Biochem. J.* **190**, 495–504.

Ceccarelli, S. M., Chomienne, O., Gubler, M., and Arduini, A. (2011). Carnitine palmitoyltransferase (CPT) modulators: A medicinal chemistry perspective on 35 years of research. *J. Med. Chem.* **54**, 3109. 10.1021/jm100809g.

Donato, M. T., Martínez-Romero, A., Jiménez, N., Negro, A., Herrera, G., Castell, J. V., O'Connor, J.-E., and Gómez-Lechón, M. J. (2009). Cytometric analysis for drug-induced steatosis in HepG2 cells. *Chemico-Biol. Interact.* **181**, 417–423.

Eberle, D., Hegarty, B., Bossard, P., Ferre, P., and Foufelle, F. (2004). SREBP transcription factors: Master regulators of lipid homeostasis. *Biochimie* **86**, 839–848.

Ensenauer, R., Fingerhut, R., Schriever, S. C., Fink, B., Becker, M., Sellerer, N. C., Pagel, P., Kirschner, A., Dame, T., Olgemoller, B., *et al.* (2012). In situ assay of fatty acid beta-oxidation by metabolite profiling following permeabilization of cell membranes. *J. Lipid Res.* **53**, 1012–1020.

Felser, A., Blum, K., Lindinger, P. W., Bouitbir, J., and Krahenbuhl, S. (2013). Mechanisms of hepatocellular toxicity associated with dronedarone–A comparison to amiodarone. *Toxicol. Sci.* **131**, 480–490.

Felser, A., Stoller, A., Morand, R., Schnell, D., Donzelli, M., Terracciano, L., Bouitbir, J., and Krahenbuhl, S. (2014). Hepatic toxicity of dronedarone in mice: Role of mitochondrial beta-oxidation. *Toxicology* **323**, 1–9.

Fischer, J. J., Michaelis, S., Schrey, A. K., Graebner, O. G., Glinski, M., Dreger, M., Kroll, F., and Koester, H. (2010). Capture compound mass spectrometry sheds light on the molecular mechanisms of liver toxicity of two Parkinson drugs. *Toxicol. Sci.* **113**, 243–253.

Fisher, E. A. (2012). The degradation of apolipoprotein B100: Multiple opportunities to regulate VLDL triglyceride production by different proteolytic pathways. *Biochim. Biophys. Acta* **1821**, 778–781.

Fromenty, B., and Pessayre, D. (1995). Inhibition of mitochondrial beta-oxidation as a mechanism of hepatotoxicity. *Pharmacol. Ther.* **67**, 101–154.

Grünig, D., Duthaler, U., and Krahenbuhl, S. (2018). Effect of toxicants on fatty acid metabolism in HepG2 cells. *Front. Pharmacol.* in press.

Grunig, D., Felser, A., Bouitbir, J., and Krahenbuhl, S. (2017). The catechol-O-methyltransferase inhibitors tolcapone and entacapone uncouple and inhibit the mitochondrial respiratory chain in HepaRG cells. *Toxicol. In Vitro* **42**, 337–347.

Guillouzo, A., Corlu, A., Aninat, C., Glaise, D., Morel, F., and Guguen-Guillouzo, C. (2007). The human hepatoma HepaRG cells: A highly differentiated model for studies of liver metabolism and toxicity of xenobiotics. *Chemico-Biol. Interact.* **168**, 66–73.

Haasio, K. (2010). Toxicology and safety of COMT inhibitors. *Int. Rev. Neurobiol.* **95**, 163–189.

Haasio, K., Koponen, A., Penttila, K. E., and Nissinen, E. (2002a). Effects of entacapone and tolcapone on mitochondrial membrane potential. *Eur. J. Pharmacol.* **453**, 21–26.

Haasio, K., Nissinen, E., Sopanen, L., and Heinonen, E. H. (2002b). Different toxicological profile of two COMT inhibitors in vivo: The role of uncoupling effects. *J. Neural Trans.* **109**, 1391–1401.

Haasio, K., Sopanen, L., Vaalavirta, L., Linden, I. B., and Heinonen, E. H. (2001). Comparative toxicological study on the hepatic safety of entacapone and tolcapone in the rat. *J. Neural Trans.* **108**, 79–91.

Haegler, P., Grünig, D., Berger, B., Krähenbühl, S., and Bouitbir, J. (2015). Impaired mitochondrial function in HepG2 cells treated with hydroxy-cobalamin[c-lactam]: A cell model for idiosyncratic toxicity. *Toxicology* **336**, 48–58.

Hoppel, C., DiMarco, J. P., and Tandler, B. (1979). Riboflavin and rat hepatic cell structure and function. Mitochondrial oxidative metabolism in deficiency states. *J. Biol. Chem.* **254**, 4164–4170.

Igal, R. A., Wang, P., and Coleman, R. A. (1997). Triacsin C blocks de novo synthesis of glycerolipids and cholesterol esters but not recycling of fatty acid into phospholipid: Evidence for functionally separate pools of acyl-CoA. *Biochem. J.* **324**, 529–534.

Jorga, K., Fotteler, B., Heizmann, P., and Gasser, R. (2001). Metabolism and excretion of tolcapone, a novel inhibitor of catechol-O-methyltransferase. *Br. J. Clin. Pharmacol.* **48**, 513–520.

Kaakkola, S. (2000). Clinical pharmacology, therapeutic use and potential of COMT inhibitors in Parkinson's disease. *Drugs* **59**, 1233–1250.

Kazantzis, M., and Stahl, A. (2012). Fatty acid transport proteins, implications in physiology and disease. *Biochim. Biophys. Acta* **1821**, 852–857.

Lew, M. F., and Kricorian, G. (2007). Results from a 2-year centralized tolcapone liver enzyme monitoring program. *Clin. Neuropharmacol.* **30**, 281–286. 10.1097/WNF.0b013e318149f290.

Longo, D. M., Yang, Y., Watkins, P. B., Howell, B. A., and Siler, S. Q. (2016). Elucidating differences in the hepatotoxic potential of tolcapone and entacapone with DILIsym((R)), a mechanistic model of drug-induced liver injury. *CPT Pharmacometrics Syst. Pharmacol.* **5**, 31–39.

Mason, T. M. (1998). The role of factors that regulate the synthesis and secretion of very-low-density lipoprotein by hepatocytes. *Crit. Rev. Clin. Lab. Sci.* **35**, 461–487.

Morand, R., Donzelli, M., Haschke, M., and Krahenbuhl, S. (2013). Quantification of plasma carnitine and acylcarnitines by high-performance liquid chromatography-tandem mass spectrometry using online solid-phase extraction. *Anal. Bioanal. Chem.* **405**, 8829–8836.

Olanow, C. W. (2000). Tolcapone and hepatotoxic effects. Tasmar Advisory Panel. *Arch. Neurol.* **57**, 263–267.

Olowe, Y., and Schulz, H. (1982). 4-Bromocrotonic acid, an effective inhibitor of fatty acid oxidation and ketone body degradation in rat heart mitochondria. On the rate-determining step of beta-oxidation and ketone body degradation in heart. *J. Biol. Chem.* **257**, 5408–5413.

Soupene, E., and Kuypers, F. A. (2008). Mammalian long-chain acyl-CoA synthetases. *Exp. Biol. Med. (Maywood, N.J.)* **233**, 507–521.

Spahr, L., Rubbia-Brandt, L., Burkhard, P. R., Assal, F., and Hadengue, A. (2000). Tolcapone-related fulminant hepatitis: Electron microscopy shows mitochondrial alterations. *Digest. Dis. Sci.* **45**, 1881–1884.

Tomoda, H., Igarashi, K., Cyong, J. C., and Omura, S. (1991). Evidence for an essential role of long chain acyl-CoA synthetase in animal cell proliferation. Inhibition of long chain acyl-CoA synthetase by triacsins caused inhibition of Raji cell proliferation. *J. Biol. Chem.* **266**, 4214–4219.

Tserng, K. Y., Jin, S. J., and Hoppel, C. L. (1991). Spiropentaneacetic acid as a specific inhibitor of medium-chain acyl-CoA dehydrogenase. *Biochemistry* **30**, 10755–10760.

Vernez, L., Hopfgartner, G., Wenk, M., and Krahenbuhl, S. (2003). Determination of carnitine and acylcarnitines in urine by high-performance liquid chromatography-electrospray ionization ion trap tandem mass spectrometry. *J. Chromatogr. A* **984**, 203–213.

Wang, G., Bonkovsky, H. L., de Lemos, A., and Burczynski, F. J. (2015). Recent insights into the biological functions of liver fatty acid binding protein 1. *J. Lipid Res.* **56**, 2238–2247. 10.1194/jlr.R056705.

Wendel, A. A., Lewin, T. M., and Coleman, R. A. (2009). Glycerol-3-phosphate acyltransferases: Rate limiting enzymes of triacylglycerol biosynthesis. *Biochim. Biophys. Acta* **1791**, 501–506.

Yan, S., Yang, X. F., Liu, H. L., Fu, N., Ouyang, Y., and Qing, K. (2015). Long-chain acyl-CoA synthetase in fatty acid metabolism involved in liver and other diseases: An update. *World J. Gastroenterol.* **21**, 3492–3498.

Zhou, L., Xu, L., Ye, J., Li, D., Wang, W., Li, X., Wu, L., Wang, H., Guan, F., and Li, P. (2012). Cidea promotes hepatic steatosis by sensing dietary fatty acids. *Hepatology* **56**, 95–107,